We are IntechOpen, the world's leading publisher of Open Access books Built by scientists, for scientists

6,900
Open access books available

186,000
International authors and editors

200M
Downloads

154
Countries delivered to

Our authors are among the

TOP 1%
most cited scientists

12.2%
Contributors from top 500 universities

CLARIVATE ANALYTICS
BOOK CITATION INDEX
INDEXED

WEB OF SCIENCE™

Selection of our books indexed in the Book Citation Index
in Web of Science™ Core Collection (BKCI)

Interested in publishing with us?
Contact book.department@intechopen.com

Numbers displayed above are based on latest data collected.
For more information visit www.intechopen.com

Chapter

Enhancement of the Magnetoelectric Effect in PZT-Ni Ferrite Composites Using Post Sintering Thermal Treatment

Rashed Adnan Islam

Abstract

In this chapter, the piezoelectric and magnetoelectric properties of Pb $(Zr_{0.52}T_{0.48})O_3$–X $NiFe_{1.9}Mn_{0.1}O_4$ (PZT-NFM, where X ranges from 3 to 10%) were investigated along with SEM and TEM analysis. Post sintering thermal treatment (annealing and aging) was introduced to enhance the piezoelectric and magneto-electric property of the composites. The density was found around 7.6–7.8 gm/cc. The piezoelectric constant d_{33} and the voltage constant were found to be decreased with increasing magnetic particle from 3–10%. Experimental results indicated that the magnetoelectric voltage coefficient (dE/dH) increases with increasing percentage of Nickel Ferrite (~35 for 3% NF to 140 mV/Oe. cm for 10% NF at 1125°C). The samples, which were annealed and aged after sintering show as high as 50% (140 to 220 mV/cm Oe) increase in dE/dH coefficient. This is due to the increase in resistivity due to better homogeneity. The H-M curve of the composite powders show that the PZT-NFM is a ferromagnetic material as well. The SEM investigation shows very compact structure with average grain size around 150 nm and some areas of the NF rich phase. The X-ray mapping shows that the NF is distributed in the big grains of the matrix and after annealing it homogenizes.

Keywords: nickel ferrite, ferromagnetic, spinel, piezoelectric, magnetoelectric, perovskite

1. Introduction

Magnetoelectric materials contains combination of the ferroic properties such as polarization, and magnetization [1–4]. Due to the interrelationship between ferroelectricity and magnetism, it is possible to control of ferroelectric properties using magnetic field and vice versa. Cr2O3, BiFeO3, YMnO3 etc. which are single phase magnetoelectric (ME) materials do not provide much benefits due to very weak magnetoelectric effect [5–7]. The solution to this issue is composites utilizing the product property of the two materials and have much better ME voltage coefficient [8–10]. Magnetoelectric (ME) particulate sintered composite can be fabricated in combination of magnetostrictive and piezoelectric phases [11–15]. Among the many advantages of sintered composites, simplicity in synthesis, cost-effective materials and fabrication process, and better control of desired geometry are the

most important ones. However, the ME effect in particulate sintered composite is still low and it is of the order of 100 mV/cm.Oe. Laminated composites which are fabricated by bonding colossus piezoelectric and magnetostrictive materials are very popular because they display excellent ME properties [16–19]. Dong et al. have shown a large response of 22 V/cm.Oe at 1 Hz using piezo fiber laminated between the high-permeability magnetostrictive FeBSiC alloy with epoxy [20]. The inherent materials property is the ferroelasticity that complemented both the ferroelectricity and ferromagnetism in same materials. This is a three-step mechanism: (a) ferroelectric ion movement needs structural building blocks, (b) super exchange type magnetic-interaction conduits and (c) the symmetry condition is satisfied [21]. One simple inference from this is that it is possible to synthesize the ferroelectric ferromagnets by replacing diamagnetic ions by paramagnetic ones on the B-site of oxyoctahedral ferroelectric perovskites.

Among the piezoelectric materials, Lead Zirconate Titanate (PZT) is the most popular for its high piezoelectric property and most importantly it shows magnetoelectric effect when used in a composite as reported by others. PZT when mixed with some magnetostrictive particles (such as ferrites) have been found to exhibit an extrinsic magnetoelectric effect resulting from a coupling interaction. The precondition to it is increased resistivity, almost zero to no interdiffusion, no chemical reaction and reduced interfacial such as microcracks and porosities [22]. Both the magnitude of magnetostriction and the slope of the magnetostriction curve with respect to applied magnetic field should have a large value in order to achieve high values of pseudo-piezomagnetic coefficients in the magnetostrictive phase [22–24]. In this regard, Ni ferrite doped with Mn ($NiFe_{1.9}Mn_{0.1}O_4$) can be promising candidate due to its increased resistivity, superior magnetization and small coercive field in order to switch the domains.

Co-firing of piezoelectric and magnetostrictive phases with mismatch in coefficient of thermal expansion and lattice at high temperature induces strain in the sintered composite. Thus, a post sintering heat treatment is necessary to homogenize the matrix grain structure, reduce the strain and remove the chemical or stress gradients at the interface. It has been shown that piezoelectric and dielectric properties of sintered ceramics improve after annealing. Annealing also enhances the magnetostrictive properties of some common ferrites such as CoFe2O4. The annealing and aging technique for this reason has been used in fabricating materials with strong permanent magnetism [25, 26]. In this case, precipitates with soft magnetic nature are dispersed in a hard magnetic matrix, resulting in one of the best hard magnets.

In this chapter, the percentage of the Ni ferrite (doped with Mn) was varied from 3 to 10% (by mole). Two different sintering temperature (1100° and 1125°C) was investigated to see the sintering behavior and the effect of ferrite percentage and sintering temperature on physical, piezoelectric and magnetoelectric properties of the particulate composite. This chapter investigates a new post sintering treatment such as the annealing and aging technique for synthesizing ME composites with the objective of achieving a strong coupling between ferroelectric and magnetic order parameters.

2. Experimental

2.1 Processing

Powders of PbO, ZrO_2 and TiO_2 (Alfa Aesar, Co. MA. USA) were mixed with alcohol and grinding media of YTZ (ϕ 5 mm, Tosoh Co. Tokyo, Japan) in a polyethylene jar for 24 hours. Similarly, NiO_2, Fe_2O_3, $MnCO_3$ was mixed and ball milled

in same the fashion for 24 hours. After ball milling the powders were dried in an oven at 80°C. Then the powders were calcined (PZT at 750°C for 2 hours and NF at 1000°C for 5 hours). After calcinations, the powders were crushed and were examined by XRD to confirm the perovskite (for PZT) and spinel (for NF) phase. Then the powders were further crushed and sieved (US mesh # 270) very fine. Then the PZT and the NF powders were mixed stoichiometrically (for 3%, 5% and 10% NF by mole) and ball milled with alcohol and grinding media for 24 hours. After ball milling the powders were dried at 80°C, crushed in a mortar and sieved in a stainless-steel sieve of #170 US mesh. Then the powders were pressed to pellets of ϕ12.7x 1.5 mm in a hardened steel die using a hydraulic press under a pressure of 15 MPa. Pressureless sintering of composites was performed with Lindberg BlueM furnace with platinum foil (0.003 in. thick) at the bottom. The sintering temperatures were 1100° and 1125°C for 2 hrs. After sintering, samples were annealed at 800°C for 10 hours followed by air cooling and then aged at 400°C for 5 hours.

2.2 Characterization

The density of the samples was measured by Archimedes principle. XRD was perfromed in a Siemens Krystalloflex 810 D500 x-ray diffractometer on samples after calcination, sintering and post sintering treatment. For the measurement of % Spinel phase, the area under the curve for the perovskite (101) peak and spinel (311) peak was measured. Then the % Spinel was found taking the percentage of the area under spinel (311) peak among the total are under these two peaks. Specimens were polished with 0.3 μm powder, thermally etched and examined under Scanning Electron Microscope (Zeiss Leo Smart SEM). The annealed and aged specimens were chemically etched in a solution of 95% H_2O, 4% HCL and 1% HF. The average grain size of the composite was determined from SEM micrograph by linear intercept. X-ray mapping was done using the same Scanning Electron Microscope. TEM of sintered samples was done by JEOL – 1200 EX Scanning Transmission Electron Microscope.

2.3 Property measurement

An Ag-Pd electrode is painted on both surfaces of the pellets and fired at 825°C for 1 hr. The electroded specimens were polled by applying a D.C. field of 2.5 kV/mm for 20 minutes in a silicone oil bath at 120°C. The piezoelectric and dielectric properties were measured by APC YE 2730A d_{33} meter and an impedance analyzer (HP 4192, Hewlett Packard Co. USA). The Curie temperature was measured from Capacitance vs. Temperature graph with the help of Multi frequency LCR meter (HP 4274 A Hewlett Packard Co. USA). The magnetoelectric property was measured in terms of variation of dE/dH coefficient with an A.C. Magnetic field and no D.C. magnetic bias. The coefficient was measured directly as response of the sample to an A.C. magnetic input signal at 3 Hz and 60 Oe amplitude. The voltage generated from the composite was measured using a charge amplifier. The output signal from the amplifier was measured with an Oscilloscope (54601A, HP Co. USA). The output voltage is converted into dielectric displacement (D = CV/A), which can also be expressed in electric field (E = $D/\varepsilon_o\varepsilon$) and then the electric field divided by A.C. magnetic field gives the magnetoelectric voltage coefficient for PZT-NF composite.

3. Results and discussion

Figure 1 shows the density variation of the piezoelectric/magnetostrictive composites sintered at 1100 and 1125°C. Both shows similar pattern. The density
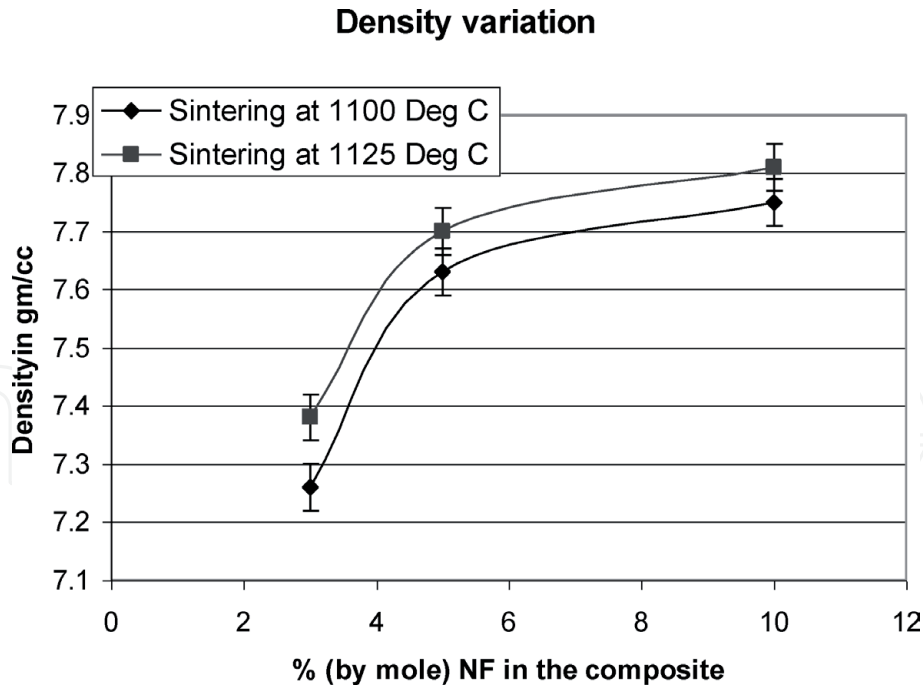
Figure 1.
Effect of % NFM on density at two different temperatures.
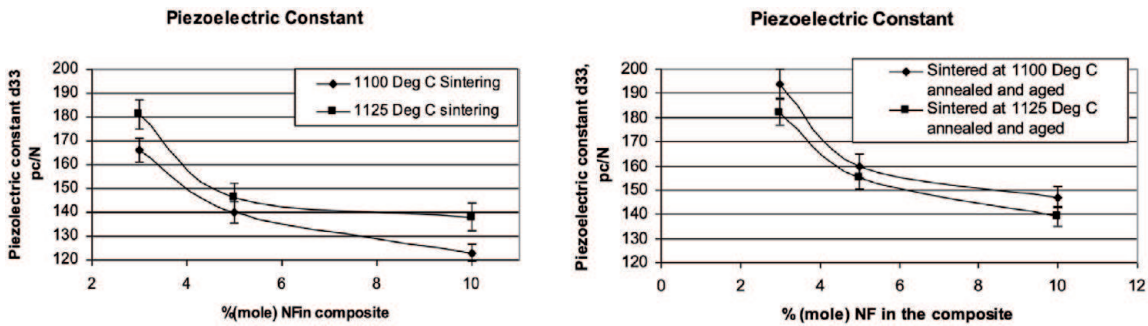

Figure 2.
Piezoelectric properties at different % NFM of sintered as well as annealed and aged samples.

increases with increasing percentage of NF and starts to plateau after 5 moles% of NFM. The samples sintered at 1125°C, showed higher densities than that of 1100°C. This is due to the better sintering behavior at higher (1125°C) temperature. **Figure 2(a)** shows the variation of the piezoelectric constant with NFM mole%. As the perovskite phase decreases with increasing NFM concentration, d33 starts to decrease. From **Figure 2(b)** an increase in d33 after annealing and aging was observed for both the sintering conditions. For the PZT-5NFM, 14% and 6% increase in d_{33} were recorded for samples sintered at 1100°C and 1125°C respectively. The difference in the magnitude of d_{33} before and after annealing and aging for other two composite samples (3% and 10% NFM) sintered at 1125°C was small. This can be associated to concurrent rise in the internal strain due to structural dissimilarity and domain size. Increase in stress decreases d33 while increase in domain size increases d_{33}. **Figure 2(c)** shows the variation of the dielectric constant with NFM concentration. The dielectric constant magnitude for the samples sintered at 1100°C showed a decrease of about 10% after thermal treatment. Based on the behavior of the piezoelectric and dielectric constant, it can be seen that the total strain magnitude remains of the same order for the samples before and after the thermal treatment.
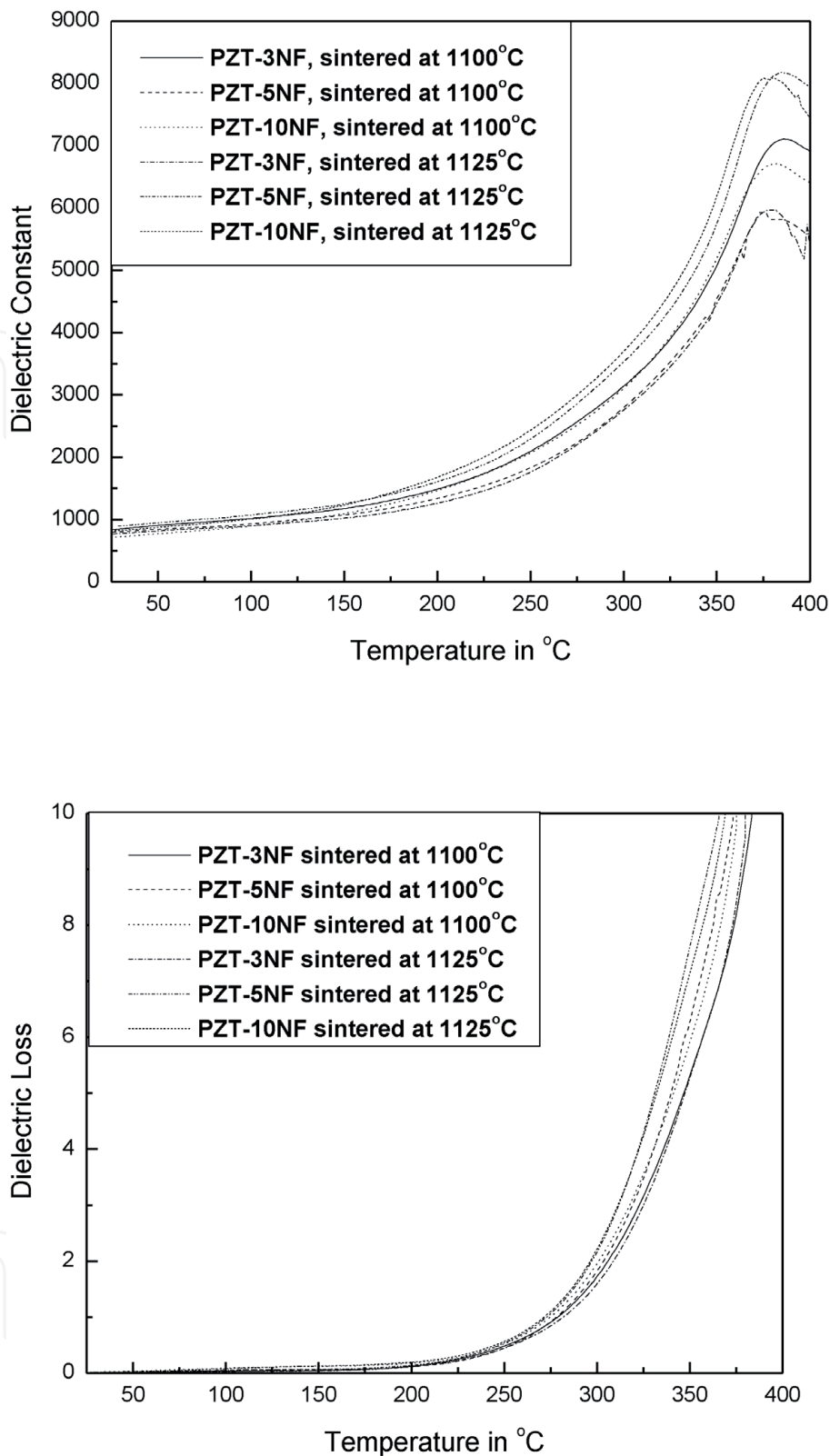
Figure 3.
Variation of dielectric constant and dielectric loss with temperature of different composition and at different sintering temperature [27–30].

Figure 3(a) and **(b)** shows the dielectric constant and loss factor as a function of temperature. The dielectric properties were measured at 1 kHz under 1 V excitation. The Curie temperature (T_{max}) measured for all the samples compositions were in the vicinity of 375°C with slight decrease in T_{max} with increasing % NFM. The loss factor ($\tan\delta$) measured was ~2% below 80°C. Beyond 200°C it increases sharply. The space charge effect and low resistivity of the PZT-NFM samples at elevated
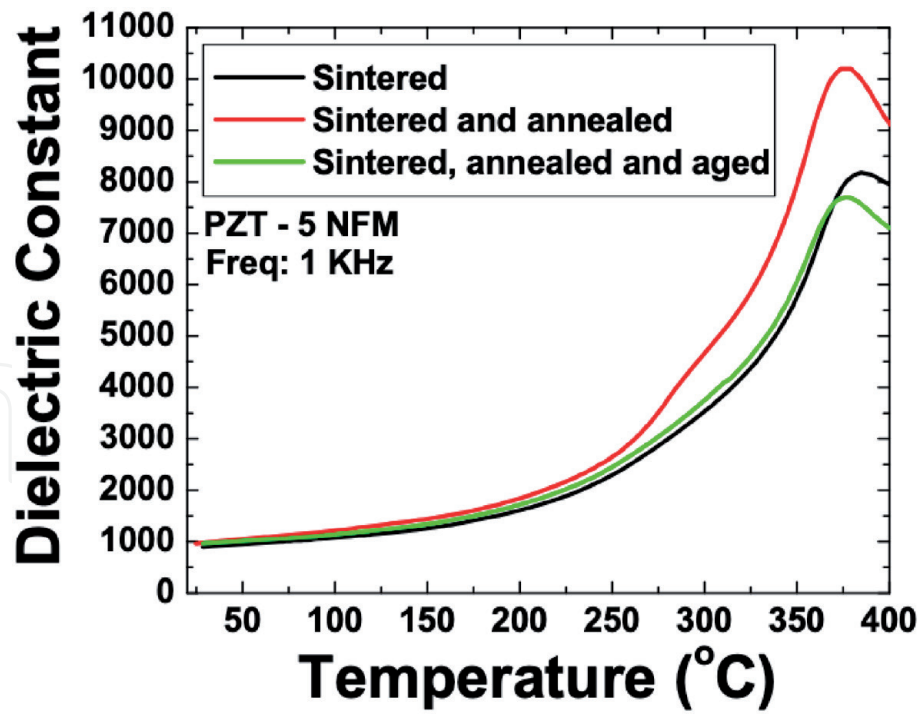
Figure 4.
Dielectric constant as a function of the temperature at 1 kHz for PZT-5 NFM at three different conditions [28, 29].
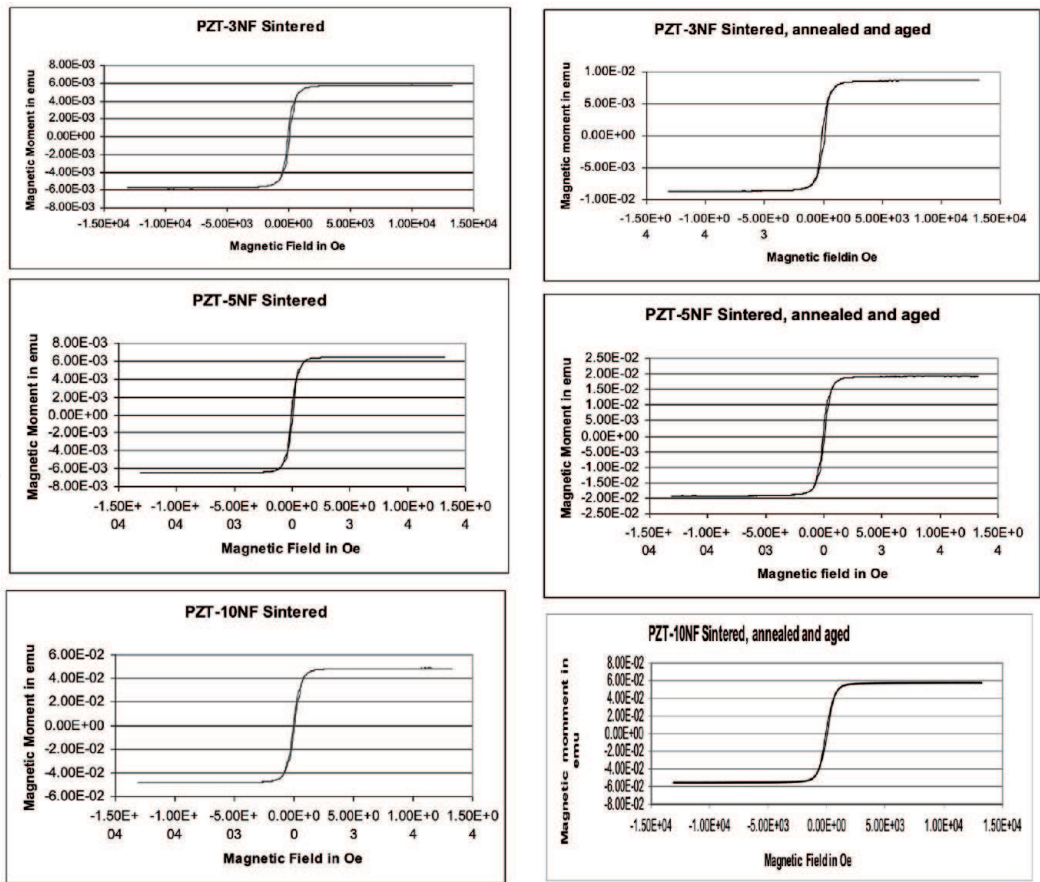

Figure 5.
Magnetic field H vs magnetic moment curve of different composite.

temperature caused the rapid rise of dielectric loss around curie temperature. The T_{max} did not change much regardless of the thermal treatment. The dielectric constant vs. temperature for PZT-5 at % NFM composites before and after different

	PZT-3NF			PZT-5NF			PZT-10NF		
	Powder	Sintered at 1100°C	Sintered and annealed	Powder	Sintered at 1100°C	Sintered and annealed	Powder	Sintered at 1100°C	Sintered and annealed
H_c (Oe)	124	86.94	89.91	97.39	75.62	78.76	109.9	69.78	70.24
M_r (µemu)	195	1010	1480	270.8	904.1	2538	219.1	5305	5575
M_s (m emu)	0.817	5.766	8.653	1.633	6.472	19.25	1.187	48.64	57.13
M_r/M_s	0.2356	0.1751	0.1711	0.1658	0.1397	0.1318	0.1846	0.1091	.0976
S	0.00575	0.005	0.0043	0.0047	0.0048	0.0036	0.0057	0.0034	0.0029
Resonance (Hz)	525	509.4	465.2	612.2	543	463	592	453.9	439.8

Table 1.
Magnetic properties of different PZT-NF powders [28].

thermal conditions were shown in **Figure 4**. The ferroelectric Curie temperature only decreased slightly (~8°C) by annealing and aging. This drop in T_{max} can be attributed to the stress relaxation which can be precisely understand by diffraction studies. During annealing as the composites were soaked in 800°C for 10 hours, grain grown occurs which can result into increased dielectric constant.

Figure 5(a) to **(f)** shows the variation of magnetic properties as a function of thermal treatment for the different composites. A substantial enrichment in remanent (M_r) and saturation (M_s) magnetization was observed after the thermal (annealing and aging) treatment. **Table 1** shows the magnetic data for the calcined powder, sintered samples and thermally treated samples. It is clearly observed that the magnetization values increased sharply after thermal treatment. No difference in coercive fields were observed between the sintered and thermally treated samples whereas remarkable differences were observed in magnetic resonance which decreased significantly after thermal treatment. These results can be explained if it is assumed that the size of spinel phase increases with the thermal treatment. As there are basic resemblance in the oxygen synchronization chemistry between the perovskite and spinel structure, it leads to the lattice dimensions that are compatible with the spinel building blocks (considering growth is along the c-axis).

Figure 6(a) shows the X-Ray diffraction patterns of composite sintered at 1125°C for 2 hrs. A pure perovskite phase was obtained with small fraction of 311 peak of spinel phase only observed for PZT-10 NFM. No other phase was detected. PZT composition of Zr: Ti = 52:48 was selected as it is closer to the morphotropic phase boundary (MPB) providing high piezoelectric property. On modification with NFM the perovskite phase was found to exhibit rhombohedral symmetry as shown by reduced splitting of 200/002 peaks. As expected, a higher sintering temperature resulted in higher content of spinel phase. **Figure 6(b)** shows the XRD pattern for same composition of samples after post sintering thermal treatment. In all three diffraction patterns, an increase in the fraction of spinel phase were clearly observed. The fraction of the spinel phase present was computed using the expression:

$$\%Spinel = \frac{Area\ under\ the\ spinel\ peak\,(311)}{Area\ under\ the\ perovskite\ peak\,\{(110)+(101)\}+Area\ under\ the\ spinel\ peak\,(311)} x\,100 \quad (1)$$
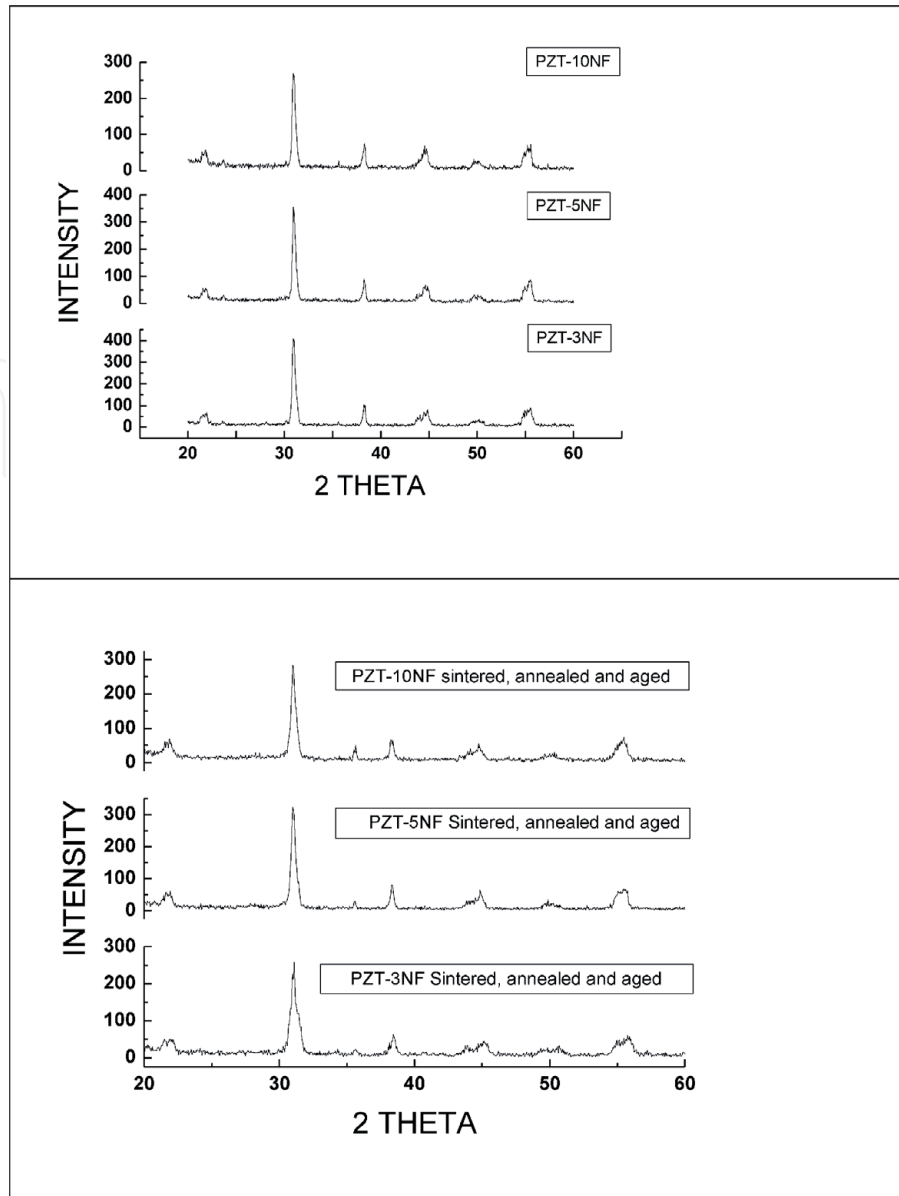
Figure 6.
XRD pattern of different compositions: a. after sintering, b. after annealing and aging.

PZT-10 NFM sintered at 1125°C showed an increase of % spinel of 1.03% (from 6.82% after sintering to 7.85% after annealing and aging). This is a significant increase considering the dissimilarity in the lattices of two phases. Comparing this result with the annealing and aging treatment, it can be theorized that there is a likelihood of homogenization in the PZT-NFM system.

Figure 7**(a)** and **(b)** shows the Magnetoelectric coefficient for 3, 5 and 10 mole% of NFM. Data are given in each figure for the three different thermal histories. For PZT-10NFM, the ME coefficient increased from 60 mV/cm-Oe after sintering to 88 mV/cm-Oe after annealing and aging which is nearly 50% increase. This is due to the reduction in misfit strain between perovskite and spinel phase, decrease in interface micro such as porosities and cracks after annealing. Reducing the interface defects, would increase the ability of piezoelectric domains to elastically react to strains induced on it by bordering magnetostrictive phases, or vice versa. To achieve high ME properties, the boundary conditions between phases needs to be as mechanically free as possible. Enhancements in the ME coefficient may also come from increased magnetization from Mn^{+3} to Mn^{+2} conversion, as an enhanced magnetic permeability has been reported to increase the effective piezomagnetic coefficient $(d\lambda/dH)$.
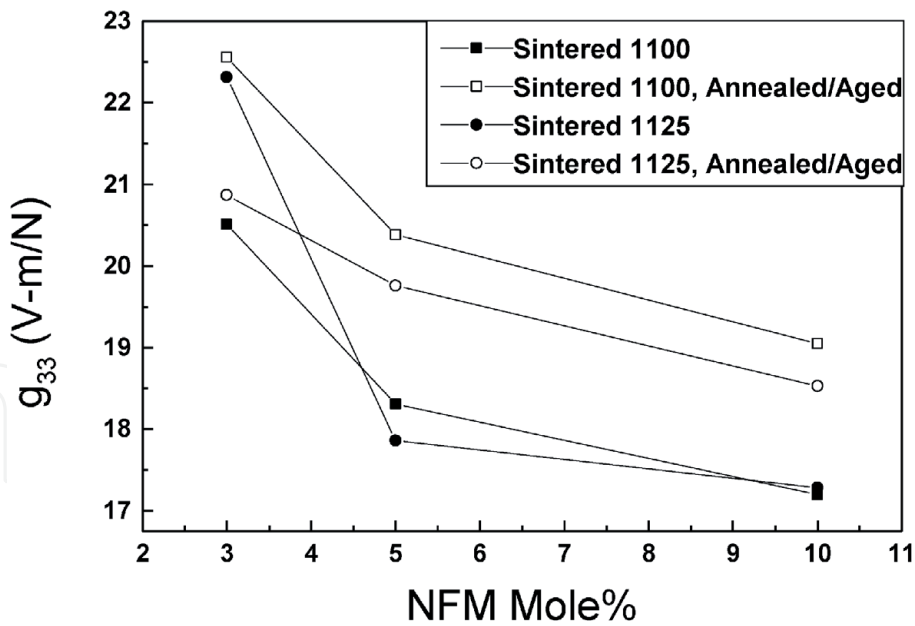
Figure 7.
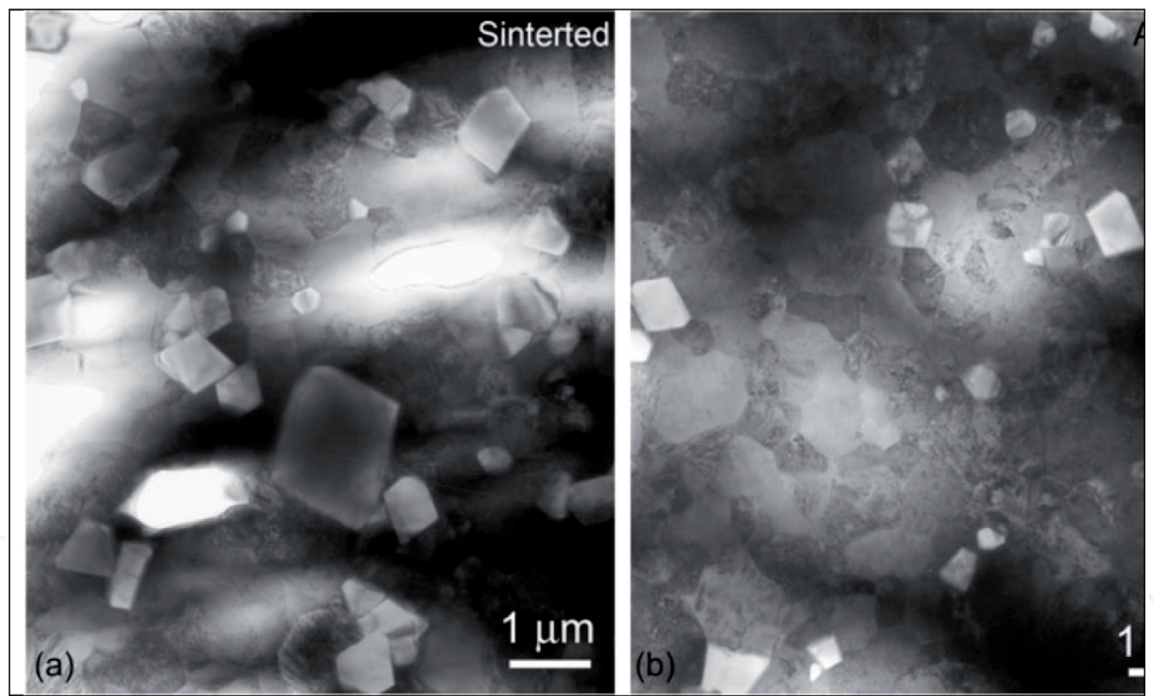*Variation of magnetoelectric coefficient as a function of % NFM [27–29].*

Figure 8.
Bright field TEM images PZT-5 NFM composites after (a) sintering, and (b) annealing [30].

Figure 8(a) shows Transmission Electron Microscopy image of as-sintered sample. This image consists of facet phases (bright contrast) NFM particles embedded in the PZT matrix. The NFM particles vary from 300 nm to 1500 nm. **Figure 8(b)** shows TEM images of annealed and aged samples. Few distinctions of microstructural characteristics fere observed from those shown in **Figure 8(a)**. The density of the NFM particles in this annealed sample is much less than that in the sintered sample. In addition, the NFM particles in the annealed sample have a typical size of 500 nm, much smaller than that in the sintered sample.

High magnification bright field TEM images of the sintered, annealed and aged samples were shown in **Figure 9(a)–(c)**. Misfit strain fields close to the
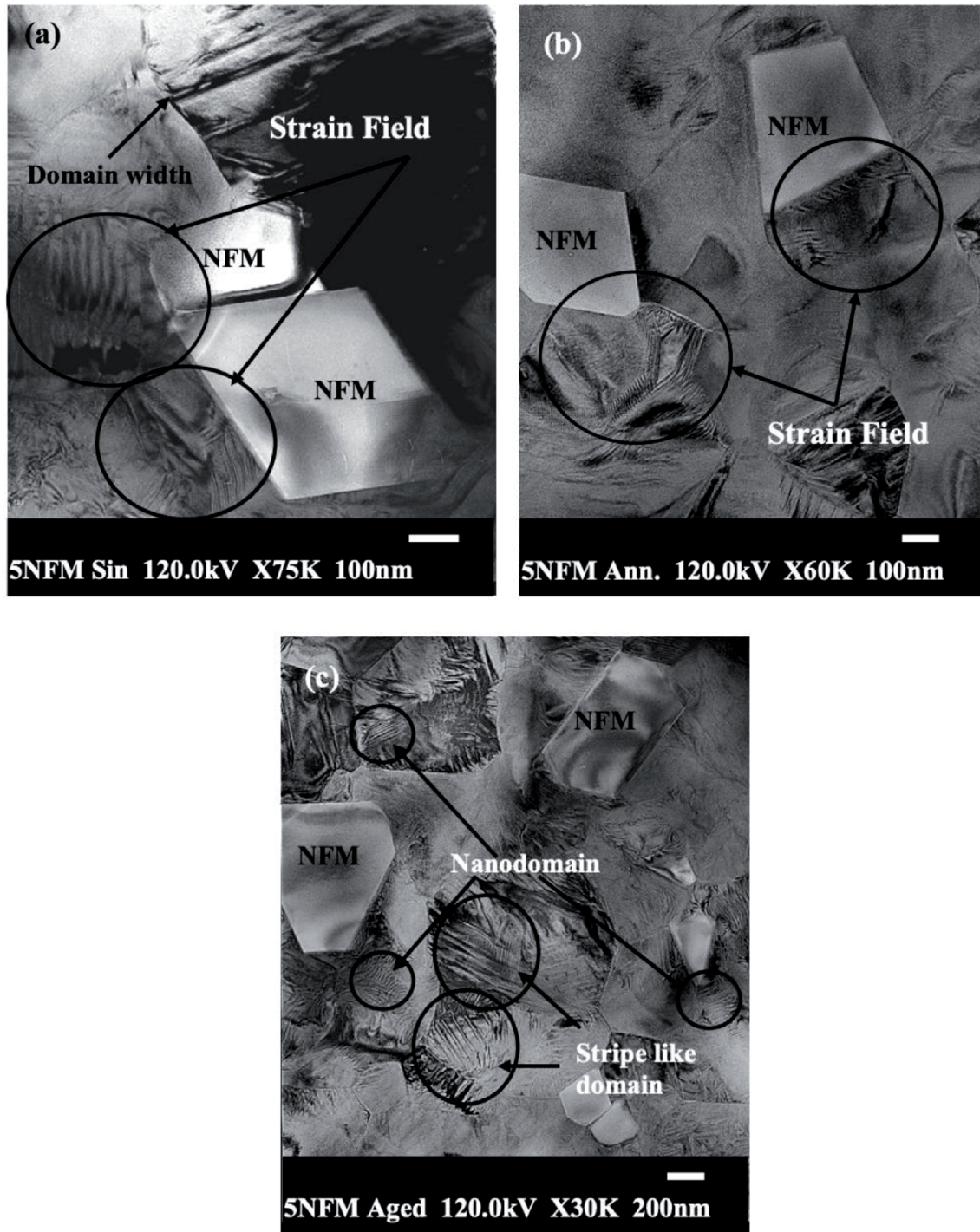
Figure 9.
Bright field TEM images PZT-5 NFM composites after (a) sintering, (b) annealing and (c) aging [30].

PZT/NFM were observed. These strain fields developed at the interface to acclimatize the mismatch in the PZT and NFM lattice. The domain patterns had larger width, which is the characteristic of 90° domains and there is intergranular discrepancy in domain width [31]. The image after annealing shows reduced misfit strain near the PZT/NFM interface. The remnant strain fields after annealing consist of additional constituent due to quenching process after annealing. Diffused grain boundaries were observed in low magnification images. The image after the aging in **Figure 9(c)** shows noticeably reduced strains. There are stripe like morphologies and they are extended from grain boundary to grain boundary. A finer scale domain structure is also observed to exist within larger domain patterns. This finer domain pattern has striation like morphology and is periodically spaced [32, 33].

4. Conclusion

In the chapter the effect of Mn doped Nickel ferrite percentage in Lead Zirconate Titanate (PZT) at different sintering temperature on the piezoelectric and magnetoelectric behavior was tried to find out and also a new post sintering treatment (annealing and aging) is introduced to enhance the magnetoelectric property. It was found that with increasing percentage of NF the piezoelectric constants, dielectric constant decreases and dielectric loss increases. The starting powder of PZT-NF (3%, 5% and 10% NF) was found ferromagnetic where the coercive field varies from 97 to 124 Oe. Post sintering treatment like annealing and aging increases the saturation magnetization M_s from 48 to 57 memu for PZT-10NF. High values (~144 mV/cm Oe) of magnetoelectric coefficient were found in 10% NF, sintered at 1125°C. The preferential distribution of NF particles in large grains of PZT matrix was found in X-ray mapping. In order to even out the distribution of NF particles and increase the magnetic phases, annealing followed by aging was introduced, as annealing is a homogenization treatment. Due to annealing the piezoelectric property increases as well as magnetoelectric coefficient. The magnetoelectric coefficient was found 211 mV/cm Oe at 3 Hz with no D.C. magnetic field bias. This is higher than any values so far reported in PZT-10% NF and sintering temperature at 1125°C. A supersaturated structure of NF in PZT is formed by annealing at high temperature followed by faster cooling. Aging allows the NF particles to distribute evenly in the structure as a different phase. The XRD pattern also shows the introduction of spinel phases in PZT matrix. The SEM images also support the grain homogenization treatment. The introduction of this post sintering treatment (annealing and aging) enhanced the property and can be further improved with optimum parameters of the treatment.

Acknowledgements

Author details

Rashed Adnan Islam
Product Integrity Engineering – Google Devices and Services, Google LLC, Mountain View, CA, United States

*Address all correspondence to: rashed@google.com

IntechOpen

References

[1] Wang J, Zheng H, Lofland SE, Ma Z, Ardabili LM, Zhao T, Riba LS, Shinde SR, Ogale SB, Bai F, Viehland D, Jia Y, Schlom DG, Wuttig M, Roytburd A, and Ramesh R (2004) Science. 303: 661.

[2] Ederer C and Spaldin N (2004) Nature Mater. 3: 849.

[3] Eerenstein W, Mathur ND, and Scott JF (2006) Nature. 442: 759.

[4] Hur N, Park S, Sharma PA, Ahn JS, Guha S and Cheong SW (2004) Nature. 429: 392.

[5] Astrov DN (1960) Sov. Phys. JETP. 11: 708.

[6] Wang J, Neaton JB, Zheng H, Nagarajan V, Ogale SB, Liu B, Viehland D, Vathiyanathan V, Schlom DG, Waghmare UV, Spaldin NA, Rabe KM, Wuttig M, and Ramesh R (2003) Science. 299: 1719.

[7] Van Aken BB, Palstra TTA, Filippetti A, and Spaldin NA (2004) Nat. Mater. 3: 164.

[8] Zheng M, Wan JG, Wang Y, Yu H, Liu JM, Jiang XP and Nan CW (2004) J. Appl. Phys. 95 (12): 8069.

[9] Ryu J, Carazo AV, Uchino K, and Kim H (2001) J. Electoceram. 7: 17.

[10] Flores VC, Baques DB, Flores DC, and Aquino JAM (2006) J. Appl. Phys. 99: 08J503.

[11] Van Suchetelene J (1972) Philips Research Report. 27: 28.

[12] Weng L, Fu Y, Song S, Tang J, and Li J (2007) Scrip. Mater. 56: 465.

[13] Ren SQ, Weng LQ, Song SH, Li F, Wan JG, and Zeng M (2005) J. Mater. Sci. 40 (16): 4375.

[14] Wu D, Gong W, Deng H, and Li M (2007) J. Phys. D: Appl. Phys. 40: 5002.

[15] Srinivasan G, DeVreugd CP, Flattery CS, Laletsin VM, and Paddubnaya N (2004) Appl. Phys. Lett. 85 (13): 2550.

[16] Ryu J, Priya S, Uchino K, Viehland D, and Kim H (2002) J. Kor. Ceram. Soc. 39: 813.

[17] Ryu J, Priya S, Uchino K, and Kim H (2002) J. Electroceram. 8: 107.

[18] Srinivasan G, Rasmussen E, Levin B, and Hayes R (2002) Phys. Rev. B 65: 134402.

[19] Dong SX, Zhai J, Li JF, and Viehland D (2006) J. Appl. Phys. 88: 082907.

[20] Dong S, Zhai J, Li JF, and Viehland D (2006) Appl. Phys. Lett. 89: 252904.

[21] J. Ryu, A.V. Carazo, K. Uchino, and H. E. Kim. Journal of Electroceramics, Vol. 7, 2001, pp. 17-24

[22] T.G. Lupeiko, S.S. Lopatin, I.V. Lisnevskaya, and B.I Zvyaginstev. Inorganic Materials Vol. 30, 1994, pp 1353-1356.

[23] C.W. Nan. Physical Review Vol. 50 (9), 1994, pp. 6082-6088.

[24] Y. X. Liu, J.G. Wan, J.M. Liu, and C. W. Nan. J. Appl. Phys. Vol. 94 (8), 2003, pp. 5118-5122.

[25] M.K. Griffiths, J.E.L. Bishop, W.J. Tucker, and H.A. Davies. J. Magnet. Magnetic Mater. 234, 331-352 (2001).

[26] Z. Sufen, J. Hanmin, W. Xuefeng, and Y. Yu. J. Magnet. Magnetic Mater. 247 [1], 15-18 (2002).

[27] R. A. Islam and S. Priya. Integ. Ferroelec. 82 (1), 1 (2006).

[28] R. A. Islam and S. Priya. Jap. J. Appl. Phys. 45 (5), L128–L131 (2006).

[29] R.A. Islam and S. Priya. J. Appl. Cer. Tech. 3(5), 353 (2006).

[30] R.A. Islam. Composition – Microstructure – Property Relationships in Dual Phase Bulk Magnetoelectric Composite [Thesis], University of Texas at Arlington, 2008.

[31] J.F. Li, X. Dai, A. Chow, and D. Viehland. J. Mater. Res. 4, 926 (1995).

[32] X. Bi, S. Chu, J. G. Zhu, and D. Laughlin. J. Appl. Phys. 99, 08B306 (2006).

[33] Z. Xu, X. Dai, D. Viehland, and D. Payne. J. Am. Ceram. Soc. 78 [8], 2220 (1999).